https://doi.org/10.5194/acp-2020-1089
Preprint. Discussion started: 22 October 2020

Atmospheric Chemistry and Physics Discussions

Impact of absorbing and non-absorbing aerosols on radiation and low-level clouds over the Southeast Atlantic from co-located satellite observations

Alejandro Baró Pérez[1,2], Abhay Devasthale[3], Frida Bender[1,2], and Annica M. L. Ekman[1,2]

[1]Department of Meteorology, Stockholm University, Stockholm, Sweden
[2]Bolin Centre for Climate Research, Stockholm, Sweden
[3]Atmospheric Remote Sensing, Research and development, Swedish Meteorological and Hydrological Institute, Norrköping Sweden

Correspondence: Alejandro Baró Pérez (alejandro.baro-perez@misu.su.se)

Abstract. We use data derived from instruments onboard the Cloud-Aerosol Lidar and Infrared Pathfinder Satellite Observation (CALIPSO) and CloudSat satellites as well as meteorological parameters from reanalysis to explore situations when moist aerosol layers overlie stratocumulus clouds over the Southeast Atlantic during the biomass burning season (June to October). One main goal is to separate and quantify the impacts of aerosol loading, aerosol type, and humidity on the radiative fluxes, including cloud top cooling. To achieve our objectives we split the data into different levels of aerosol and moisture loadings. By using the aerosol classification available from the CALIPSO products, we also separate and compare situations with pristine air, with smoke, and with other (mixed) types of aerosols. We find a substantial number of cases with mixed aerosols above clouds that occur under similar meteorological conditions as the smoke cases. In contrast, the meteorology is substantially different for the pristine situations, making a direct comparison with the aerosol cases ambiguous. The moisture content is enhanced within the aerosol layers, but we do not find a monotonous increase of the relative humidity with increasing aerosol optical depth. Shortwave (SW) heating rates within the moist aerosol plumes increase with increasing aerosol loading and are higher in the smoke cases compared to the mixed cases. However, there is no clear correlation between moisture changes and SW absorption. Cloud top cooling rates tend to decrease with increasing moisture within the overlying aerosol layers, but the influence is relatively weak and confounded by the strong variability of the cooling rates caused by other meteorological factors (most notably cloud top temperature). No clear influence of aerosol type or loading on cloud top cooling rates is detected. We also do not find any correlation between aerosol loading and the thermodynamic structure of the atmosphere nor the cloud top height, i.e. no indication of a semi-direct aerosol effect. This result is consistent with previous studies that examined clearly separated aerosol and cloud layers (in our case at least 0.4 km).

1 Introduction

Stratocumulus clouds have a cooling effect on Earth's climate due to their strong reflection of incoming solar radiation and their relatively small effect on the outgoing longwave radiation. The clouds tend to form under statically stable low tropospheric conditions and they are mainly maintained by longwave radiative cooling at the cloud top (Klein and Hartmann, 1993). The

https://doi.org/10.5194/acp-2020-1089
Preprint. Discussion started: 22 October 2020

Atmospheric Chemistry and Physics Discussions

cloud top cooling creates turbulent overturning that mixes the boundary layer and allows the cloud to be fed by moisture from the surface. It also helps to preserve the temperature inversion immediately above the cloud top (Wood, 2012). Dark-coloured aerosols, for example from biomass burning, efficiently absorb solar radiation (direct effect). This absorption alters the radiative fluxes and modifies the stability of the atmosphere, which in turn can effect cloud development and precipitation (semi-direct aerosol effect). Studies have shown that when absorbing aerosols are located above stratocumulus cloud decks, the shortwave heating of the aerosol layer tends to strengthen the inversion, which reduces the entrainment of dry air and leads to a moistened boundary layer with an increased liquid water content and more persistent clouds (Deaconu et al., 2019; Brioude et al., 2009; Johnson et al., 2004). On the contrary, if the absorbing aerosols are located within a cloud layer, they can reduce moisture and liquid water content via local shortwave heating, causing a reduction of the stratocumulus cloud cover (Deaconu et al., 2019; Hill et al., 2008). In addition to the direct and semi-direct effects, absorbing aerosols can also act as cloud condensation nuclei (CCN) and affect the radiative properties and lifetime of the clouds (indirect effects, Twomey (1977); Albrecht (1989)). The overall climate impacts of the rich set of interactions between absorbing aerosols, clouds and radiation are not yet well understood and consequently not well represented by large-scale models (Deaconu et al., 2019). Model differences in aerosol and cloud properties lead to disagreeing forcing estimates, especially in regions where aerosols and clouds overlap (Zhang et al., 2019; Schulz et al., 2006).

From June to October, large amounts of biomass burning aerosols emitted by wildfires in the southwestern African Savanna are transported westwards over the Southeast Atlantic Ocean (De Graaf et al., 2020; Deaconu et al., 2019; Ichoku et al., 2003). The anticyclonic circulation typical of this region causes a broad area of subsidence over the cool waters of the upwelling zone in the ocean, producing one of the largest stratocumulus cloud decks on the planet (Formenti et al., 2019; Klein and Hartmann, 1993). Under usual conditions, the biomass burning aerosols are mostly advected over the marine boundary layer and hence above the stratocumulus clouds (Adebiyi et al., 2015). As these aerosols typically contain large amounts of soot (Chazette et al., 2019), the biomass burning season in the Southeast Atlantic offers an excellent opportunity to study the complex interactions between absorbing aerosols and clouds and to characterise their manifestations. Several studies have used satellite observations to investigate situations with absorbing aerosols above clouds. Some of them have analysed these situations on a global scale (e.g. Devasthale and Thomas (2011); Kacenelenbogen et al. (2019)) whereas others have focused on the Southeast Atlantic (e.g. Wilcox (2010); Costantino and Bréon (2013); Adebiyi et al. (2015); Deaconu et al. (2019)). The studies focused on the Southeast Atlantic have shown that an increase in the amount of absorbing aerosols above clouds results in a cloud fraction increase (Costantino and Bréon, 2013) and that the clouds are optically thicker in situations with high aerosol loadings (Deaconu et al., 2019). However, when using satellite observations, it is a complicated task to isolate the effects of aerosols on clouds from those caused by the background meteorology due to covariations between aerosols and meteorological conditions. The biomass burning aerosols are usually accompanied by an enhanced humidity associated with the outflow from the continental boundary layer (Haywood et al., 2004; Adebiyi et al., 2015; Zhou et al., 2017; Deaconu et al., 2019). The moisture, besides its potential impacts in the aerosol ageing (Dubovik et al., 2002; Haywood et al., 2004; Kar et al., 2018; Deaconu et al., 2019), can also remotely affect the underlying clouds through the modification of radiative fluxes. For instance, large-eddy simulations and radiative transfer calculations have shown a reduction of the stratocumulus top longwave

https://doi.org/10.5194/acp-2020-1089
Preprint. Discussion started: 22 October 2020


Atmospheric Chemistry and Physics Discussions

(LW) cooling due to a downward LW flux increase caused by the water vapour accompanying the aerosol layer (Yamaguchi et al. (2015), Zhou et al. (2017) and Deaconu et al. (2019)). This effect, combined with an increase of the atmospheric stability due to shortwave (SW) absorption by the aerosols may decrease the entrainment rate (Deaconu et al., 2019), which impacts the deepening of the boundary layer and the transition from stratocumulus to cumulus (Wood, 2012).

In this work we use four years (2007-2010) of recently updated satellite datasets to further explore situations when moist aerosol layers overlie stratocumulus clouds in the Southeast Atlantic. We use retrievals derived from instruments onboard the Cloud-Aerosol Lidar and Infrared Pathfinder Satellite Observation (CALIPSO) and CloudSat satellites as well as meteorological parameters from the ERA5 reanalysis (Hersbach et al., 2020). We also use the CALIPSO aerosol discrimination algorithm to analyse the composition of the aerosol layers and to compare smoke versus non-smoke aerosol occurrences. One main goal of our study is to separate and quantify the impacts of aerosol loading, aerosol type, and humidity on the radiative fluxes within the aerosol layer as well as their potential influence on cloud top cooling. More specifically, we seek observational support for the model-based finding of reduced cloud top cooling from moist aerosol layers above the boundary layer. Furthermore, we examine if the loading and type of aerosol affect general cloud features such as cloud top height. In our study we use the satellite data products to select cases where aerosols and clouds are separated from each other. This was not explicitly done by Deaconu et al. (2019), who in their analysis included all aerosols above clouds occurrences close to the coast of Angola. Another novel feature of our study is that we explore if the previously observed covariance between aerosol and moisture in the region implies a consistent and monotonous increase of humidity with aerosol loading. The observational data and methodology are described in Section 2. Our results are presented in Section 3 followed by a summary and conclusions in Section 4.

2 Datasets and methodology

2.1 CALIPSO, Cloudsat and ERA5

Table 1 displays a summary of the datasets, products and variables used in the study. The CALIOP (Cloud-Aerosol Lidar with Orthogonal Polarization) instrument on board CALIPSO provides information on aerosol and cloud optical properties with high vertical resolution. Furthermore, the CALIPSO V4 classification algorithm (Kim et al., 2018) discriminates between different types of aerosols and clouds into ice or water phase (Winker et al., 2009). The aerosol type is determined using measurements of the integrated attenuated backscatter and the volume depolarization ratio as well as surface type and aerosol layer altitude (Omar et al., 2009). The ice-water phase is derived from the volume depolarization that allows to discriminate between the spherical cloud droplets and nonspherical ice crystals (Winker et al., 2009). An aerosol extinction-to-backscatter ratio (aerosol lidar ratio) is assumed in order to enable, in most cases, the calculation of extinction from lidar backscatter signals (Winker et al., 2009).

Two datasets were used from the CALIPSO Version 4.20 (V4) Level 2 product: the Merged Aerosol and Cloud Layers Data and the Aerosol Profile Data. In the Merged Aerosol and Cloud Layers Data the information is reported by layers at a 5 km horizontal resolution. We used it in order to know the altitudes of the aerosol and cloud layers as well as the aerosol types. The full set of tropospheric aerosol types identified by the algorithm are: clean marine, dust, polluted continental/smoke,

https://doi.org/10.5194/acp-2020-1089
Preprint. Discussion started: 22 October 2020

Atmospheric Chemistry and Physics Discussions

clean continental, polluted dust, elevated smoke and dusty marine. It is important to highlight that “elevated smoke" refers to smoke layers with tops higher than 2.5 km above the ground level (approximation of the region above the planetary boundary layer (PBL) (Kim et al., 2018)), whereas “polluted continental/smoke" can include smoke if the aerosol layer top is below 2.5 km, because the similarity in the optical properties between both aerosol types (smoke and polluted continental) makes them indistinguishable within the PBL (Kim et al., 2018).

The Aerosol Profile Data provides information as profiles with 60 m and 5 km of vertical and horizontal resolution, respectively and includes vertically resolved meteorological information derived from the Modern-Era Retrospective analysis for Research and Applications, Version 2 (MERRA-2). From this data set, we obtained: profiles of temperature and pressure, used in the computation of the potential temperature for exploring the stability of the atmosphere, profiles of relative humidity (RH), to examine the correlation between moisture above clouds and aerosol loadings as well as the aerosol extinction and column optical depth of tropospheric aerosol, which both are related to the aerosol type and aerosol loading. The Cloud Profiling Radar (CPR) onboard CloudSat produces detailed images of cloud structures. The profiles of radiative fluxes and atmospheric heating rates usesd in our study were obtained from the 2B-FLXHR-LIDAR product (Henderson et al., 2013), which combines aerosol and cloud profiles from CALIPSO and CloudSat, weather data from the European Centre for Medium-Range Weather Forecasts (ECMWF), a dynamic land surface model (Lebsock et al., 2017) and radiative transfer model to compute the profiles of radiative fluxes at a vertical resolution of 240 m (Lebsock et al., 2017).

To carry out the analysis, the products obtained from the Merged Aerosol and Cloud Layers Data and the Aerosol Profile Data from CALIPSO were combined with the radiative fluxes and atmospheric heating rates obtained from CloudSat. Since the spatial resolution between the satellite data sets differ, the CloudSat profiles were averaged to the 5 km horizontal resolution of CALIPSO. Finally, the ERA5 reanalysis (Hersbach et al., 2020) was used to characterize the governing meteorological conditions during the period of analysis with special emphasis on winds.

2.2 Area and time period

The Southeast Atlantic area selected for the study extends from 10 to 18°S and from 2 to 10°E. It is located over the Namibian stratus region identified by Klein and Hartmann (1993) and is close to the continent, where the biomass burning aerosol loadings are high and where the aerosol layer is on average centered above the low-level clouds (Deaconu et al., 2019). The final extent of the area of study was determined based on a balance between having a sufficient number of cases while keeping the natural variability of meteorology and cloud properties relatively small. Our area of study is similar to the one used by Deaconu et al. (2019), but it is shifted 4° towards the west so that the entire domain is over the ocean. It is also 3° longer in the north-south direction.

The time period selected for the study is June to October for the years 2007 to 2010, i.e. covering the July-October period when the dominant winds frequently transport biomass burning aerosols from continental sources towards the stratocumulus decks located over the Southeast Atlantic (Adebiyi et al., 2015). Following Deaconu et al. (2019), who studied June to August (JJA) of one year (2018), we also included the month of June. Here, we divide the full biomass burning season into two parts,

https://doi.org/10.5194/acp-2020-1089
Preprint. Discussion started: 22 October 2020

Atmospheric Chemistry and Physics Discussions

Table 1. Satellites and models used in the study. Variables with a star (*) are derived from the Modern-Era Retrospective analysis for Research and Applications, Version 2 (MERRA-2) data product.

Satellite/reanalysis	Products and variables	Resolution
CALIPSO	**Merged Aerosol and Cloud Layers Data**: -Aerosol top and base altitudes (km) -Cloud top altitudes (km) -Aerosol type. **Aerosol Profile Data Products**: -Extinction Coefficient at 532 nm -Column Optical Depth Tropospheric Aerosols at 532 nm -Temperature* -Relative Humidity* -Pressure*	Horizontal: 5 km Vertical: 60 m
CloudSat	**2B-FLXHR-LIDAR product**: -Radiative fluxes -Atmospheric heating rates	Vertical: 240 m
ERA5	wind speed and direction	Horizontal: 31 km

comparing the JJA period studied by Deaconu et al. (2019) with the September-October (SO) period, as a means of investigate how differences in meteorological conditions impact the manifestation of aerosol-cloud interactions.

2.3 Selection and classification of cases

To study the effects of aerosols overlying clouds, we identify and contrast cases with and without aerosols above clouds. We also distinguish between cases with smoke aerosols and aerosols with other optical properties using the CALIPSO V4 Level 2 product on aerosol and cloud layers (cf. Section 2.1) as follows:

1. **Smoke cases**: Atmospheric columns in which aerosol layers(s) classified by the CALIPSO V4 algorithm as “elevated smoke" are above and detached from clouds. The main characteristics of these cases are:
   - The presence of only one cloud layer in the atmospheric column with cloud top altitude between 0.75km and 2.5km. Cases with cloud top altitudes lower than 0.75km are not considered to avoid the ground cluttered data in CloudSat retrievals, whereas the maximum altitude (2.5km) was chosen to only capture scenarios with shallow clouds.
   - The presence of one or more aerosol layers above the cloud layer with a separation between the cloud layer and the bottom aerosol layer in the range 0.4 to 6km. With the lower distance we expect to reduce the number of situations with possible contact between aerosols and clouds, whereas the higher altitude was selected to discard situations in

https://doi.org/10.5194/acp-2020-1089
Preprint. Discussion started: 22 October 2020


Atmospheric Chemistry and Physics Discussions

which aerosols are very far from the clouds. Situations with more than one aerosol layer above cloud are included only if the distance between the aerosol layers is smaller than 0.3 km.

2. **Mixed cases**: Cases with aerosol layer(s) that are *not* categorized as “elevated smoke" by the CALIPSO V4 algorithm. Otherwise, the same criteria as for the smoke category are used for the selection of the altitudes and number of aerosol and cloud layers.

3. **Pristine cases**: Cases containing only a cloud layer with a cloud top altitude between 0.75km and 2.5km, i.e. the same characteristics as described for the smoke cases (above) but with no aerosol present above the cloud layer.

3 Results

In this section, we will first examine the composition of the aerosol layer as determined by the CALIPSO V4 retrieval algorithm. Thereafter, we will examine if and how the spatial and temporal distribution of the aerosol and cloud layers differ between the three groups of cases (as defined in Section 2.3) and to what extent differences in the prevailing meteorological conditions may prevent a fair comparison between them. Finally, we will analyze the influence of the aerosol layer and its composition on the radiative heating profiles and examine the main drivers of any influence (aerosol type, loading or RH).

3.1 Aerosol type occurrence

The frequency of occurrence for the different aerosol types found within the aerosol layers are shown in figure 1. The “elevated smoke", which corresponds to the smoke cases in our study, is the predominant type, representing 53% and 58% of the total aerosol layers found during JJA and SO, respectively. Among the remaining aerosol types (which correspond to the mixed cases in our study), the “Polluted continental/smoke" is predominant. Furthermore, the number of cases classified as “Elevated smoke" and “Polluted continental/smoke" is greater during SO than JJA. This happens because during September, there is a maximum in the extent of the stratocumulus deck at the same time as there is a maximum in transport of continental aerosol over the Southeast Atlantic due to a strengthening of the anticyclone over southern Africa (Adebiyi et al., 2015).

Figure 1 shows that during the biomass burning season there is a non-negligible number of "mixed" aerosol cases overlying the stratocumulus clouds over the Southeast Atlantic. The possibility exists of having some of these cases misclassified as not being smoke for two reasons: first, some of the "mixed" cases can indeed contain a substantial amount of smoke, if the smoke is located below 2.5 km (cf. section 2.3); second, the CALIPSO algorithm itself can misclassify the aerosol type under certain circumstances (Kim et al., 2018), although the aerosol classification was improved from version V3 to V4 (used here) of the algorithm, resulting in an increase of the aerosol classified as smoke over the Southeast Atlantic (Kar et al., 2018).

https://doi.org/10.5194/acp-2020-1089
Preprint. Discussion started: 22 October 2020

Atmospheric Chemistry and Physics Discussions

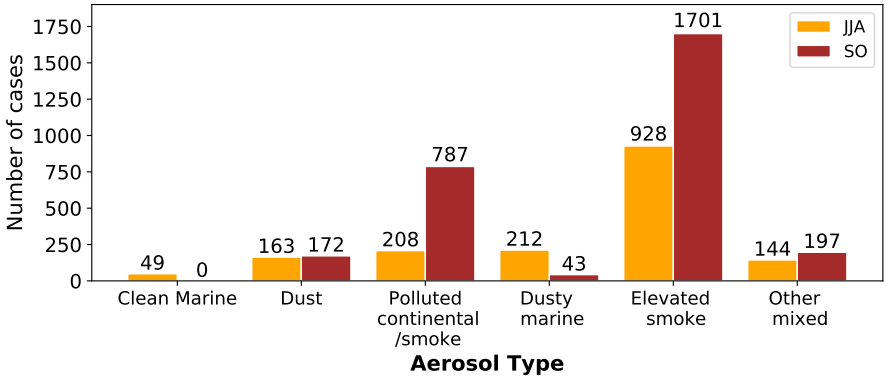

Figure 1. Aerosol types found in aerosol layers fulfilling the selection criteria (section 2.3) during the months June-July-August (JJA) and September-October (SO) during the period 2007-2010. “Other mixed" refers to situations with more than one aerosol layer, where one of the layers is not defined as “elevated smoke". Our smoke cases correspond to “elevated smoke" whereas our “mixed cases" contains the rest of the aerosol types.

Table 2. Number of days and profiles used in the analysis for each case. Details on the definition of the cases are found in section 2.3

Periods analysed during years 2007-2010	Number of days (number of columns) analysed.		
	Smoke	mixed	pristine
June-July-August (JJA)	30 (1028)	32 (751)	20 (503)
September-October (SO)	46 (1812)	47 (1107)	5 (120)

3.2 Temporal and spatial distribution of cases

Next, we examine the number of cases identified and their spatial (horizontal and vertical) distributions during the two periods (JJA and SO). If these characteristics differ substantially, then the cases may also be subjected to different meteorological conditions which may influence the outcome of any comparison.

Table 2 shows the total number of days and the total number of profiles when “smoke", “mixed" and “pristine" cases were found. The number of aerosol profiles is greater during SO than during JJA for the reasons explained in section 3.1. In contrast, pristine profiles are more frequent during JJA than SO.

The longitudinal and latitudinal distributions of all profiles are shown in Figure 2. In general, the horizontal distributions are similar between the two aerosol cases (except perhaps the latitudinal distributions in SO), which is beneficial for a comparison between them as it indicates similar meteorological conditions (cf. also Section 3.3). In contrast, the pristine cases show clearly different horizontal distributions. During both periods, all groups (smoke, mixed and pristine) tend to have more cases

https://doi.org/10.5194/acp-2020-1089
Preprint. Discussion started: 22 October 2020

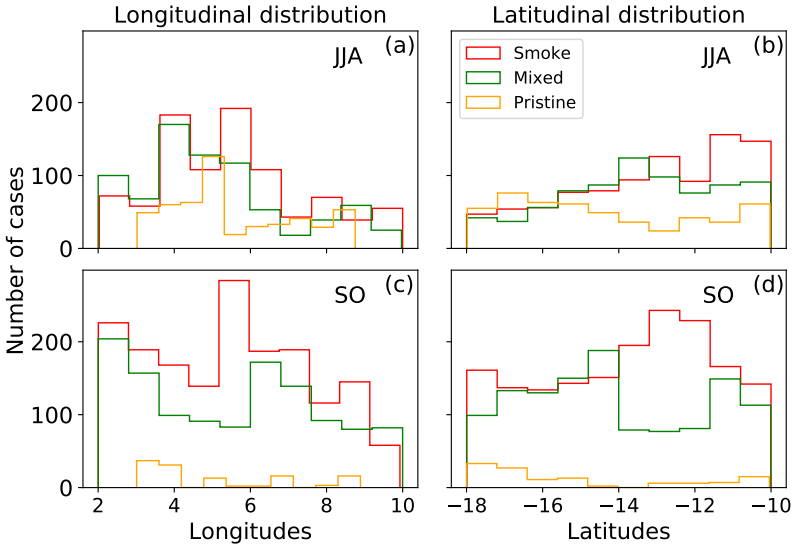

Figure 2. Latitudinal and longitudinal distributions of the cases analysed during June-July-August (JJA)(a-b) and September-October (SO)(c-d) in the period 2007-2010.

at longitudes between 2 and 6°E, which means that more profiles matching the conditions described in Section 2.3 were found away from the coast rather than near the coast.

The altitudes of the tops of the cloud layers are shown in Figure 3 together with the top and base altitudes of the aerosol layers. The average altitude of the cloud tops is clearly higher in the pristine cases (between 1.3 and 1.4 km) compared to both aerosol cases (around 1 km). When an aerosol layer is present above a cloud layer, the maximum cloud top altitude is 1.7 km (one smoke case in JJA), but in general there were very few cases with cloud tops higher than 1.5 km, a result consistent with Wilcox (2010). In contrast, the maximum cloud top altitude for the pristine cases is close to 1.9 km. Another notable feature is that the aerosol layer altitudes are on average higher during SO (4.2 km for smoke and 4.0 km for mixed cases) than during JJA (3.3 km for smoke and 2.9 km for mixed cases). Deaconu et al. (2019) obtained a similar result when comparing the periods May-July and August-October (with the later period having higher aerosol layer altitudes) for the years 2006 to 2010. We also note that all smoke cases have aerosol top altitudes higher than 2.5 km in accordance with the characteristics of the CALIPSO V4 aerosol type “elevated smoke".

A likely cause of the difference in aerosol altitudes between JJA and SO is the location of the Southern African Easterly Jet. This jet supports biomass burning aerosol transport from the continent to the ocean and is stronger and migrates to higher altitudes (between 650 and 600 hPa) during SO (Adebiyi and Zuidema, 2016). Another factor that could contribute to the observed differences in the location of the aerosol layer is that land surface temperatures are higher in October (southern

https://doi.org/10.5194/acp-2020-1089
Preprint. Discussion started: 22 October 2020

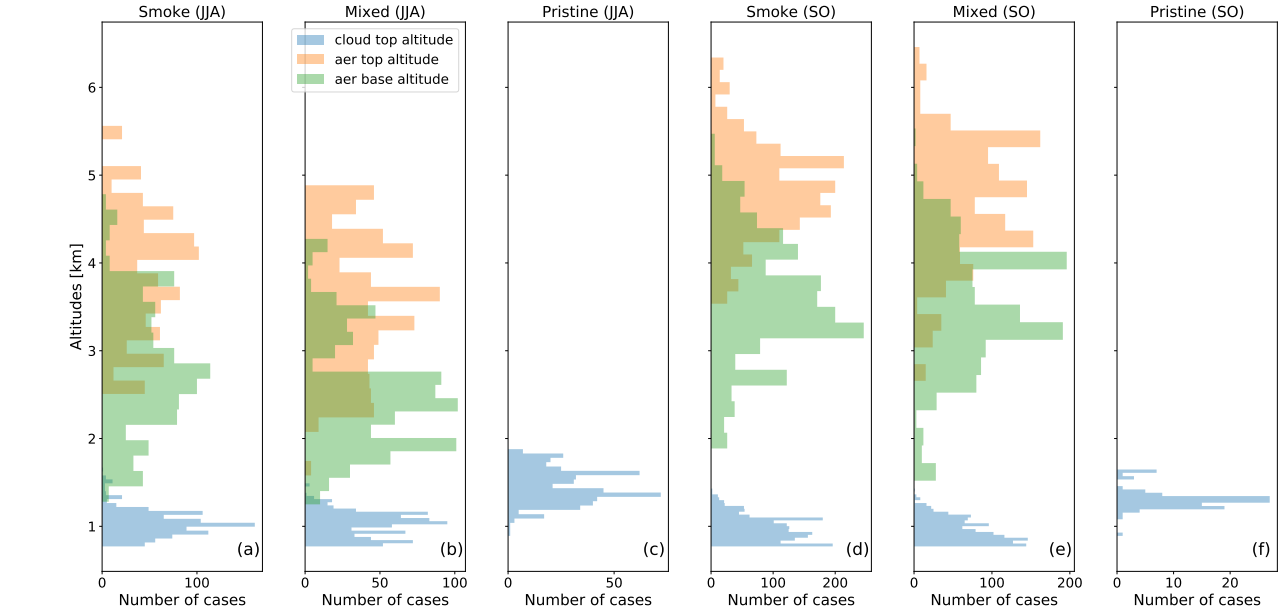

Figure 3. Altitudes of the cloud top and the aerosol (aer) top and base layers during June-July-August (JJA) and September-October (SO) in the period 2007-2010. Aerosol cases are subdivided into smoke and mixed using the CALIPSO discrimination algorithm for the aerosol type.

hemispheric spring) than in June (winter). Consequently, the top of the boundary layer, and the injection heights, may also be higher.

3.3 Prevailing meteorological conditions

195 The atmospheric circulation governs the thermodynamic environment where clouds form. Even a small perturbation in the prevailing wind pattern may affect the temperature and humidity profiles and thereby the characteristics of a stratocumulus cloud layer (Wood, 2012). It is therefore important to ensure that the different groups of cases are subjected to similar large-scale circulation patterns and meteorology when investigating any influence of aerosol layers on the radiative fluxes and low-level cloud properties.

200 Figure 4 shows the average horizontal wind direction for all three groups of cases at a level representative of the cloud layer (900 hPa during both JJA and SO) and a level representative of the aerosol layer (700 and 625 hPa during JJA and SO, respectively, cf. Figure 3). The smoke and mixed cases have almost identical wind patterns, which is expected since they were often detected during the same days and since their temporal and spatial distributions were found to be similar (Section 3.2). At 900 hPa, southeasterly winds dominate during both JJA and SO. At 700 (625) hPa, the anticyclonic circulation imposes 205 winds from the northeast (east) in JJA (SO), which favours transport of continental aerosol over the domain. The winds are clearly different for the pristine cases. In the free troposphere, the anticyclonic circulation is shifted northwards and winds

https://doi.org/10.5194/acp-2020-1089
Preprint. Discussion started: 22 October 2020


Atmospheric Chemistry and Physics Discussions

blow predominantly from the open ocean during both JJA and SO, preventing aerosol advection over the area of study. The average winds also differ within the cloud layer (at 900hPa); the pristine cases have a more southerly component compared to the two aerosol cases. Based on the analysis of the large-scale wind patterns, we draw the conclusion that the smoke and mixed aerosol cases experience similar large-scale circulation conditions while the pristine cases do not. Figure 4, together with a closer look at the wind speeds (not shown), also confirms that winds are stronger during SO compared to JJA, which is in agreement with the strengthening of the land-based anticyclone during SO and the strenghtening and migration to higher altitudes of the Southern African Easterly Jet (Adebiyi et al., 2015; Adebiyi and Zuidema, 2016).

Figure 5 displays the average profiles of aerosol extinction, RH and temperature for the different cases. The extinction is higher for the smoke than for the mixed cases. At aerosol layer altitudes, the northeasterly-easterly winds observed in figure 4 bring additional moisture together with aerosol resulting in higher RH values in the presence of aerosols above clouds compared to the pristine cases. This confirms previous studies associating the presence of aerosols above clouds with high moisture at aerosol layer altitudes in the region (e.g. Adebiyi et al. (2015); Deaconu et al. (2019)). Higher RH values are also observed in SO compared to JJA which can be linked to the strengthening of the easterlies during SO. During JJA, the RH within the aerosol layer is up to 8.5% higher for the smoke than for the mixed cases. The maximum difference in RH between the aerosol cases reduces to only 3.4% just above the boundary layer during SO. Even though RH differences are small, extinction differences reach 0.05 which is close to the peak average extinction of the mixed cases (0.06) in SO. The potential temperature profiles show a shallower boundary layer with a stronger inversion in the presence of aerosols compared to the pristine situations which supports the cloud top heights differences observed in figure 3. It is likely that the difference in boundary layer height and cloud top altitudes is mainly caused by the northward shift of the anticyclonic circulation for the pristine cases (Figure 4).

In summary, while the two aerosol cases have similar meteorological conditions, the pristine cases differ in terms of winds at 700 hPa, temperature and RH profiles. These differences constitute an obstacle to detect any aerosol influence on cloud properties and radiative fluxes when comparing aerosol versus pristine cases. This needs to be kept in mind in the following subsection.

3.4 Radiative heating profiles

Figure 5 (a-b) shows the average radiative heating profiles for the different cases. The main difference between the smoke and mixed cases in net radiation is found within the aerosol layer, where the smoke cases show a clear average heating during both JJA and SO while the mixed cases only show an average heating during SO. The differences in net heating is mainly caused by a difference in the SW fluxes as the differences in the LW fluxes are small. Within the cloud layer, the net radiative heating for the pristine cases is similar in magnitude compared to the aerosol cases. However, the similar magnitude is a result of higher values of both SW heating and LW cooling. Above the boundary layer, the SW aerosol absorption is relatively small for the pristine cases. The LW cooling is also smaller than for the two aerosol cases, but still, the net radiative heating is always negative.

The average heating rates are sensitive to variations in the altitudes of the individual aerosol and cloud layers. We therefore identify the maximum LW cooling in the cloud layer (as a proxy for cloud top cooling) and the maximum SW heating in

https://doi.org/10.5194/acp-2020-1089
Preprint. Discussion started: 22 October 2020

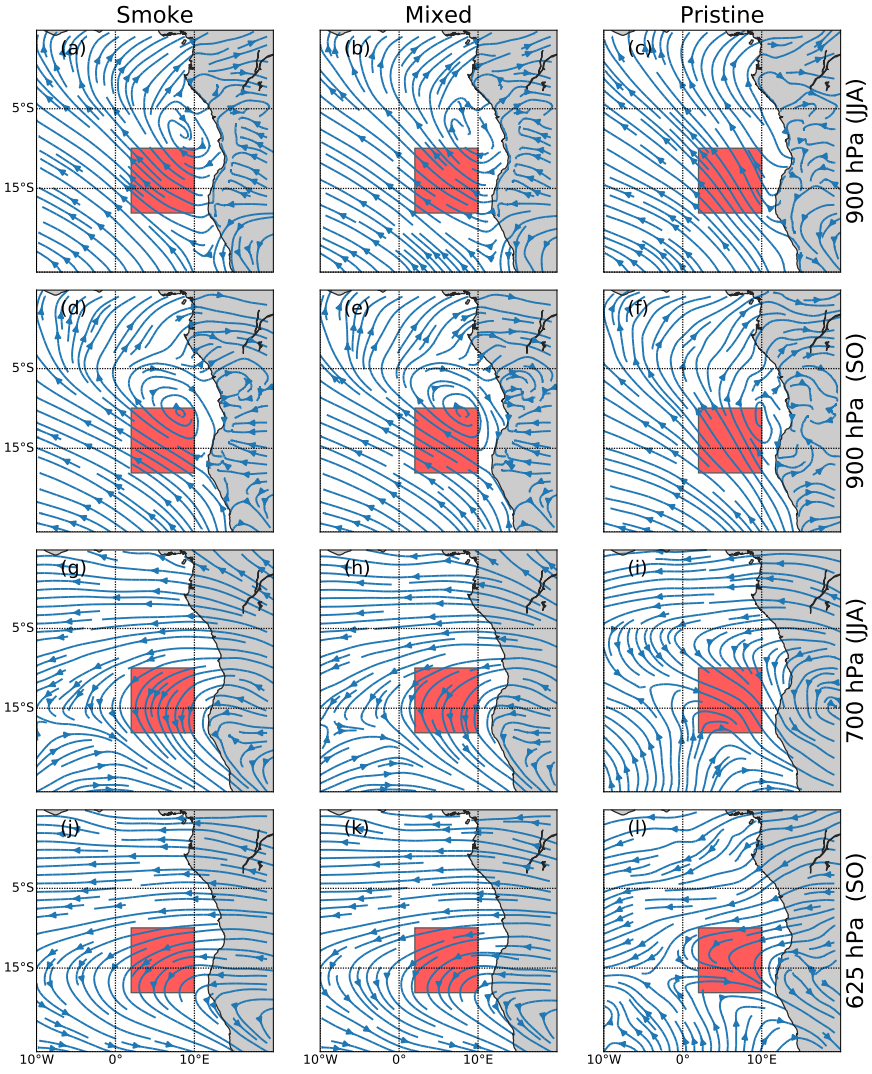

Figure 4. Streamlines corresponding to the average horizontal wind speed at 900 hPa (representative levels of cloud) in JJA and SO, and 700 (625) hPa (representative levels of aerosols) in JJA (SO) during the days when the smoke, mixed aerosol and pristine cases were identified during the period 2007-2010. The red square corresponds to the area study.

the aerosol layer for each profile in each case and compare their distributions as box plots (figure 5). No clear difference is observed in the cloud top cooling rates between the aerosol cases, while the values of the median, first and third quartiles are substantially lower for the pristine cases. A likely reason for the difference between the aerosol and pristine cases is the difference in cloud top heights (cf. Figure 3 and discussion in Section 3.5). The mean maximum SW heating within the aerosol layer is on average higher in the smoke cases than in the mixed cases. The spread in the heating rates is also larger which is

https://doi.org/10.5194/acp-2020-1089
Preprint. Discussion started: 22 October 2020

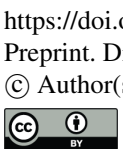

Atmospheric Chemistry and Physics Discussions

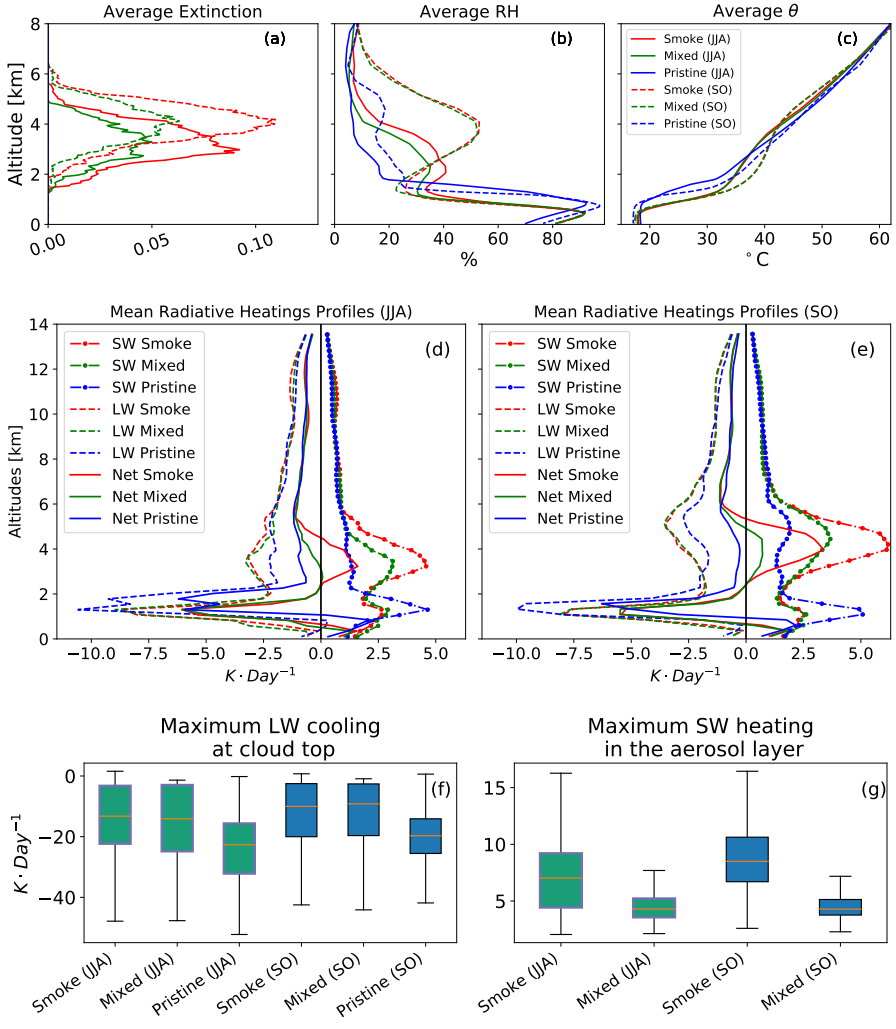

Figure 5. (a-c) Mean profiles of aerosol extinction, relative humidity (RH) and potential temperature (θ) for the smoke, mixed and pristine cases during June-July-August (JJA) and September-October (SO) during the period 2007-2010. (d-e) Mean shortwave (SW), longwave (LW) and net (Net) radiative heating profiles for the same cases and periods. (f-g) Box plots showing maximum, minimum, median, first and third quartiles of the maximum LW cooling at cloud top (f) and the maximum SW heating in the aerosol layer (g) for the smoke, mixed and pristine cases.

consistent with the wider aerosol optical depth (AOD) range observed in the smoke cases compared to the mixed cases (cf. Figure 6)

https://doi.org/10.5194/acp-2020-1089
Preprint. Discussion started: 22 October 2020

Atmospheric Chemistry and Physics Discussions

3.5 Influence of aerosol loading and relative humidity on heating profiles

In this subsection we will focus on the smoke and mixed cases and examine to which extent variations in RH and aerosol loading affects the SW heating within the aerosol layer. Similarly, we will investigate if moisture and AOD variations have a significant effect on the LW cooling rates at cloud top.

In this subsection we will focus on the smoke and mixed cases and examine to which extent variations in RH and aerosol loading affects the SW heating within the aerosol layer. Similarly, we will investigate if moisture and AOD variations have a significant effect on the LW cooling rates at cloud top.

To account for differences in aerosol loading, each group of aerosol cases was divided into three AOD intervals (low, middle and high), with intervals chosen to give an even distribution of the number of profiles in each bin. The interval limits are different for each period (JJA and SO) and for each case since the AOD range varies in time and the smoke cases have a wider range of AOD values compared to the mixed cases (cf. Section 3.4). Figure 6 shows that the average extinction in the aerosol layer always increases with increasing AOD while there is no straight-forward relation between the AOD and average RH within the plume. During JJA, the average RH increases with increasing AOD for both groups of cases (smoke and mixed). In contrast, during SO, the highest AOD interval is instead associated with the lowest RH range. Accordingly, the Spearman's rank correlation coefficient (S) between the AOD and average RH (within the aerosol layer) is positive (S=0.34 for the smoke and S=0.21 the for mixed cases) during JJA and negative in SO (S=-0.21 for the smoke and S=-0.26 for the mixed cases). The correlation values are statistically significant (p-value$<$0.05) for both periods and both groups of cases. Thus, a higher (lower) AOD does not necessarily imply a higher (lower) RH. The radiative heating profiles for the highest and lowest AOD intervals together with the distributions of maximum SW heating within the aerosol layer and LW cooling at cloud top are shown in Figure 7. The AOD values and the aerosol type both have a distinct impact on the SW heating; the SW heating increases significantly with increasing AOD and is higher for the smoke than for the mixed cases. In contrast, the LW cooling at cloud top does not show a clear relation with the AOD level or the aerosol type. None of the cases or time periods show a clear difference in the average potential temperature profiles between the three aerosol loading levels (Figure 6). There is also no clear relation between the AOD and the cloud top altitude (S-values between -0.15 and 0.21).

To investigate the effects of the humidity of the aerosol layer on the atmospheric heating profiles we instead divide our aerosol cases into three intervals based on the average RH within the aerosol layer. The average radiative heating profiles as well as the distributions of maximum SW heating within the aerosol layer and LW cooling at cloud top are shown as a function of RH in Figure 8. The average profiles of extinction, RH and temperature are provided as supplementary information (Figure A1). There is no clear relationship between RH and SW heating rates within the aerosol layer; the Spearman's rank correlation coefficients are relatively low and also vary in sign for the smoke cases. The average LW cooling at cloud top decreases slightly (less cooling) with increasing RH within the aerosol layer, but the Spearman's rank correlation values are low suggesting a small influence. The LW cooling at cloud top is inevitably dependent on cloud top altitude (CTA) as the cloud top temperature is strongly linked to the CTA. In our data, we also observe a clear increase in cloud top LW cooling with increasing CTA (S-values between 0.36 and 0.51). It is therefore relevant to examine if the relation between the LW cooling and the RH occurs

https://doi.org/10.5194/acp-2020-1089
Preprint. Discussion started: 22 October 2020

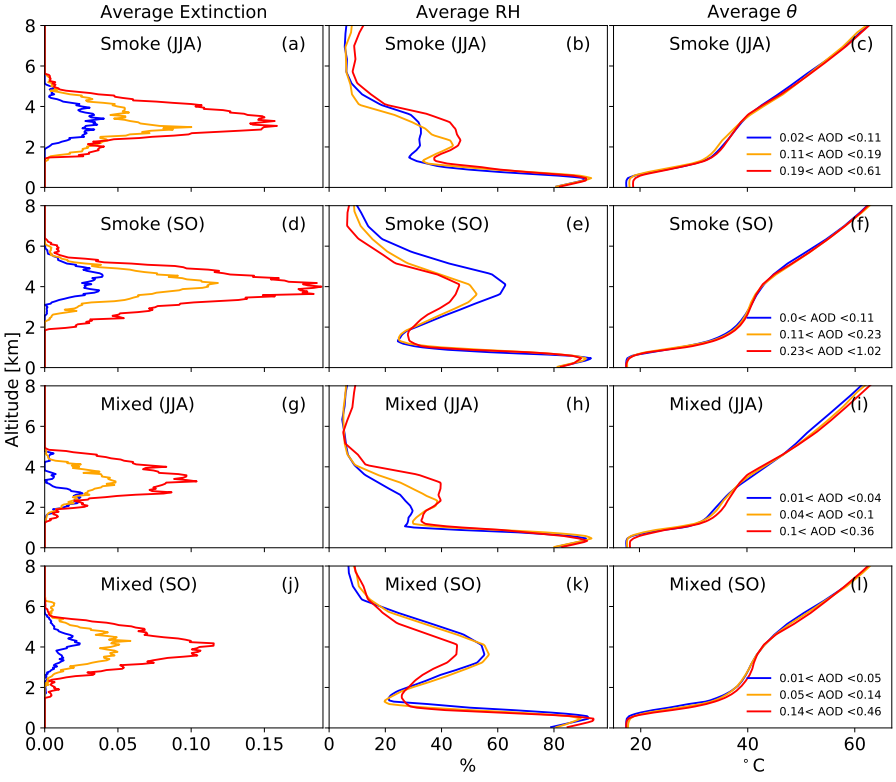

Figure 6. Mean profiles of aerosol extinction, relative humidity and potential temperature for the smoke and mixed cases during the months June-July-August (JJA) and September-October (SO). Cases are subdivided into three intervals (each one contains approximately 33 percent of the data) depending on the aerosol optical depth (AOD) value.

via an influence on the CTA. However, we find no clear relation between the CTA and the RH (S-values below 0.09 and mostly non-significant). On the other hand, Figure 9 shows that CTA variations explain an important part of the variability of the cloud top LW cooling within a certain RH interval, illustrating the difficulty in isolating a signal of the RH impact on the cloud top radiative cooling. Note that in Figure 9, both periods and aerosol cases have been combined in order to obtain a sufficient number of data points for each interval.

4 Summary and conclusions

We have used CALIPSO and CloudSat retrievals for the years 2007-2010 to study situations when moist aerosol layers overlie low-level clouds over the Southeast Atlantic during the biomass burning season (June - October). We divided our data into two periods, June-July-August (JJA) and September-October (SO) to reduce the effect of seasonal meteorology changes on the

https://doi.org/10.5194/acp-2020-1089
Preprint. Discussion started: 22 October 2020

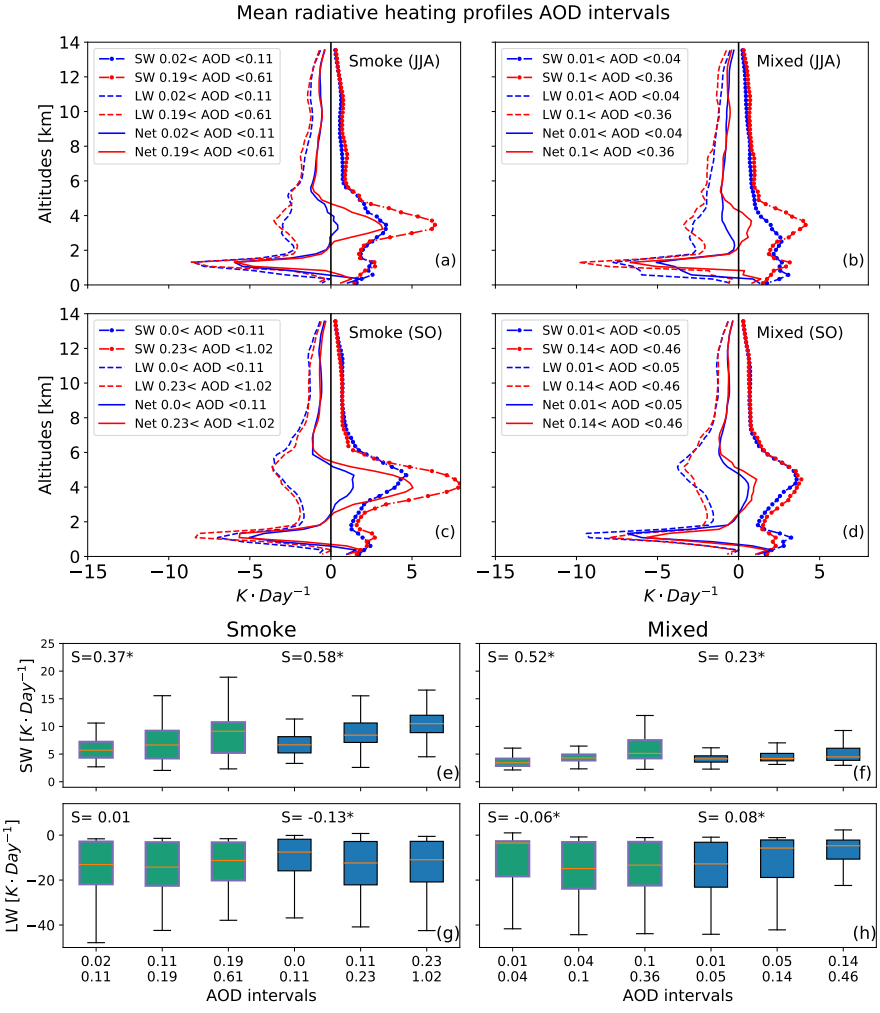

Figure 7. (a-d) Mean shortwave (SW), longwave (LW) and net (Net) radiative heating profiles for the smoke and mixed cases with high and low AOD during June-July-August (JJA) and September-October (SO) for the period 2007-2010. (e-h) Box plots of maximum SW heating within the aerosol layer (e-f) and maximum LW cooling at cloud top (g-h) for three AOD intervals for the smoke and mixed cases. Green boxes correspond to JJA and blue boxes to SO. For each case and period the Spearman's rank correlation coefficient (S) between the full range of AOD values and the SW (or LW) fluxes appears on top. Significant correlations (with p-value < 0.05) are marked with a star (*).

studied aerosol-cloud interactions. Furthermore, we used the CALIPSO V4 aerosol classification algorithm to separate cases with pristine air above clouds, smoke aerosols above clouds and other types of (mixed) aerosols above clouds.

The pristine cases displayed a clear difference in the large-scale wind pattern compared to the other two types of cases with aerosols above clouds. Easterly winds predominated in the smoke and mixed aerosol cases, which is also a prerequisite for bringing polluted continental air over the studied region, while the pristine cases were dominated by winds from the open ocean

https://doi.org/10.5194/acp-2020-1089
Preprint. Discussion started: 22 October 2020

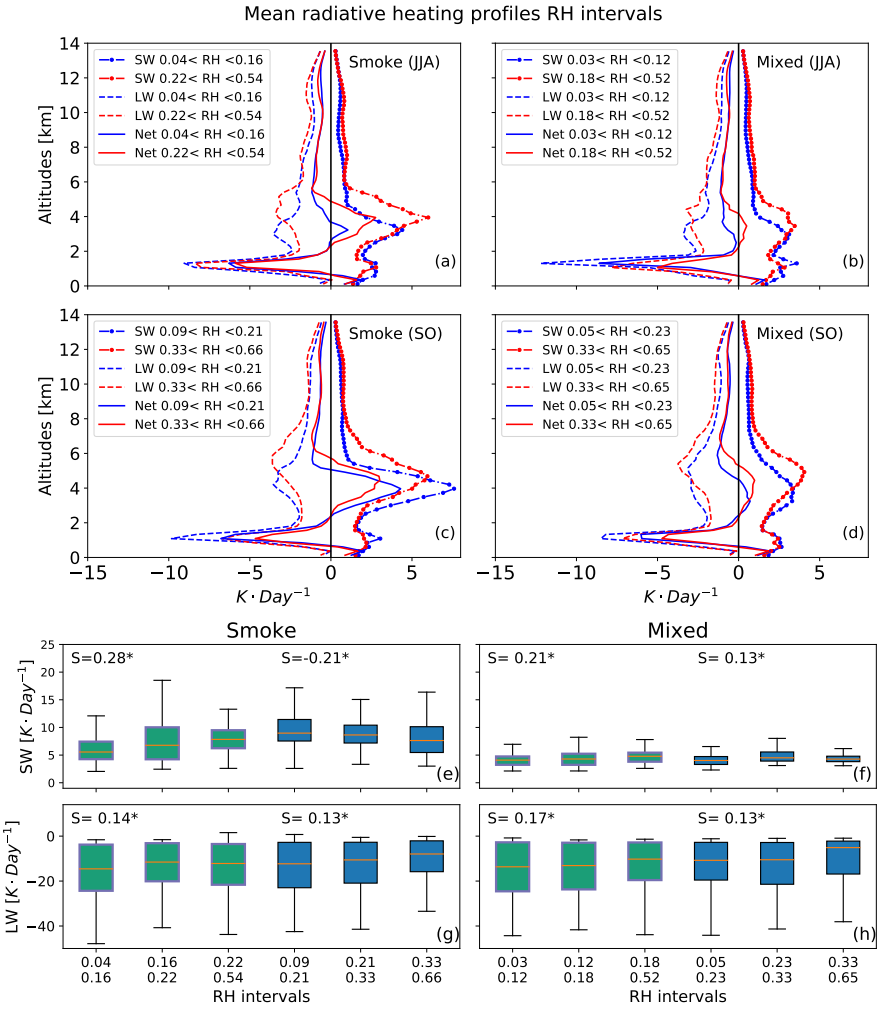

Figure 8. (a-d) Mean shortwave (SW), longwave (LW) and net (Net) radiative heating profiles for smoke and mixed cases with high and low RH June-July-August (JJA) and September-October (SO) of the period 2007-2010. (e-h) Box plots of SW heating in the aerosol layer (e-f) and LW cooling at cloud top (g-h) for three RH intervals. Right (left) panels correspond to the smoke (mixed) cases. Green boxes correspond JJA and blue boxes to SO. For each case and period the Spearman correlation coefficient (S) between the full range of RH values and the SW (or LW) fluxes appears on top. Significant correlations (with p-value < 0.05) are marked with a star (*).

(cf. Fuchs et al. (2017); Deaconu et al. (2019)). Consequently, it was not possible to conclude if any of the observed differences in low-level cloud properties (e.g. cloud top height) or thermodynamic properties of the atmosphere (e.g. stratification) between the pristine and aerosol cases were caused by the presence of an aerosol layer or by the differences in large-scale circulation. The two aerosol cases (mixed and smoke) displayed similar large-scale winds. They were both also associated with enhanced
300 levels of moisture in the free troposphere, which is typical for biomass burning plumes that are advected from the continent

https://doi.org/10.5194/acp-2020-1089
Preprint. Discussion started: 22 October 2020

Atmospheric Chemistry and Physics Discussions

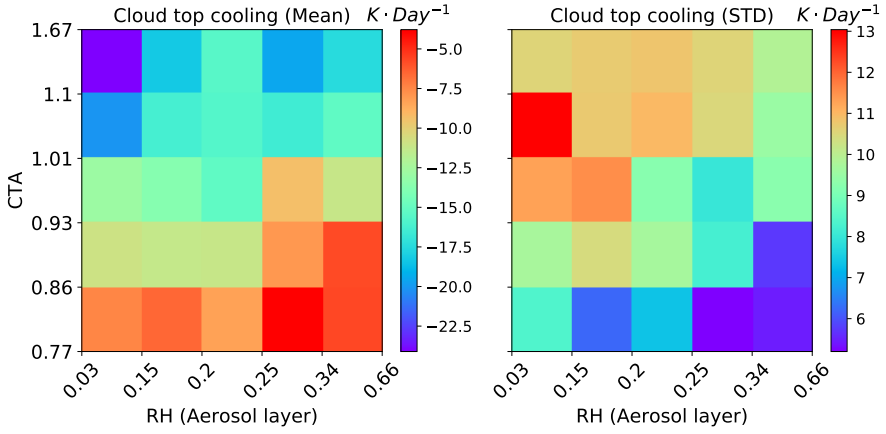

Figure 9. Histograms of the mean and the standard deviation (STD) of the maximum SW heating at the aerosol layer and the minimum LW cooling at the cloud layer as functions of CTA and RH. Both periods (JJA and SO) and both aerosol cases (smoke and mixed) were used.

(Haywood et al., 2003; Adebiyi et al., 2015; Deaconu et al., 2019). However, we did not find a monotonous increase of the RH of the aerosol layer with increasing AOD. In fact, we found a significant and negative correlation between AOD and RH during SO.

According to the CALIPSO V4 aerosol classification algorithm, and in agreement with our expectations, smoke was the dominant aerosol type overlying the stratocumulus clouds during the biomass burning season. Nevertheless, a substantial amount of other kinds of aerosols were also detected within the pollution plumes. One explanation for the obtained result cloud be that the CALIPSO algorithm miss-classifies some of the smoke aerosols as other aerosols. Another explanation could be that other aerosol types than smoke indeed occasionally dominate the pollution plumes. Chazette et al. (2019) observed a mixture of different aerosol types, mostly polluted dust and smoke, in the free troposphere over the coastal regions of Namibia (near the area of our study) during the biomass burning season. Their results are consistent with our findings and merits a broader definition of the pollution plumes overlying the stratocumulus clouds.

Our analysis clearly showed that the SW heating of the aerosol layer increased with higher aerosol loading and that the heating rates were higher in the smoke cases compared to the mixed aerosol cases. Changes in the RH of the aerosol layer always had a negligible impact on the SW heating rates, in agreement with the findings by Yamaguchi et al. (2015) and Deaconu et al. (2019). We found no clear impact of changes in AOD or aerosol type on the thermodynamic structure of the atmosphere nor the cloud top height, i.e. no indication of a semi-direct aerosol effect. Previous studies have suggested that there is a weak overall semi-direct effect of elevated smoke layers over the Southeast Atlantic and that the gap between the absorbing aerosol layer and the underlying cloud must be small (less than 0.5 km) to detect a significant influence (Herbert et al., 2020; Costantino and Bréon, 2013; Adebiyi and Zuidema, 2018). Our results are consistent with these studies as we selected cases with a minimum distance of 0.4 km to avoid any potential contact between the aerosol layer and the cloud.

https://doi.org/10.5194/acp-2020-1089
Preprint. Discussion started: 22 October 2020


Atmospheric Chemistry and Physics Discussions

No impact of the aerosol loading or type on the cloud top radiative cooling rates was found. For smoke, this result is expected since smoke aerosols do not absorb in the LW part of the spectrum (Yamaguchi et al., 2015). There was a weak tendency of decreasing (less negative) LW cooling rates with increasing RH within the overlying aerosol layers, but differences were small and confounded by the strong variability in the cooling rates. Deaconu et al. (2019) calculated that an increase in the water vapor content of the aerosol layer from “low" to “high" could dampen the net cloud top cooling by about $5 K day^{-1}$. This is a small number compared to the variability of the LW cooling rates found in our analysis within one single RH interval. It shows the difficulty of detecting the impact of RH changes within the aerosol layer on the underlying clouds and the need to carefully constrain the meteorology.

Data availability. CALIPSO products (CAL_LID_L2_05kmMLay-Standard-V4-20 and CAL_LID_L2_05kmAPro-Standard-V4-20) were obtained from the Atmospheric Science Data Center (ASDC) website: urlhttps://asdc.larc.nasa.gov/project/CALIPSO, last access: 19 October 2020. Cloudsat product 2B-FLXHR-LIDAR.P2_R04 was obtatined from the Cloudsat Data Processing Center website: http://www.cloudsat.cira.colostate.edu/order-data, last access: 19 October 2020. ERA5 datasets were obtained from the Climate Data Store website: https://cds.climate.copernicus.eu/cdsapp#!/dataset/reanalysis-era5-pressure-levels?tab=form, last access: 19 October 2020.

Author contributions. The original idea of the study came from AMLE with input from ABP, AD and FAM. ABP performed the data analysis and provided all visualizations and wrote the initial paper draft. AD provided assistance with the satellite retrievals. ABP, AMLE, FB and AD analysed the results. ABP wrote the paper with input and revisions from AMLE, FB and AD.

Competing interests. The authors declare that they have no conflict of interest.

Acknowledgements. This study was funded by the Swedish National Space Agency grant 16317. The data analysis was performed on resources provided by the Swedish National Infrastructure for Computing (SNIC) at the National Supercomputing Centre at Linköping University.

https://doi.org/10.5194/acp-2020-1089
Preprint. Discussion started: 22 October 2020

Atmospheric Chemistry and Physics Discussions

Appendix A: Supplementary material

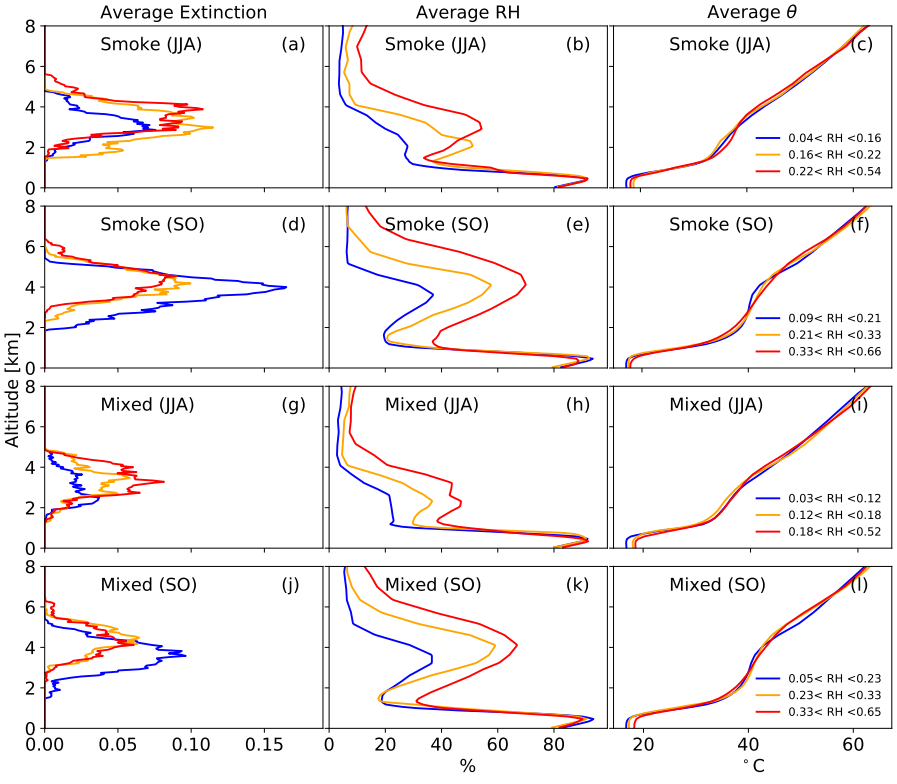

Figure A1. Mean profiles of aerosol extinction, relative humidity and potential temperature for the smoke cases June-July-August (JJA) and September-October (SO). Cases where subdivided into 3 intervals (each one approximately is the 33 percent of the data) depending on the AOD value.

https://doi.org/10.5194/acp-2020-1089
Preprint. Discussion started: 22 October 2020

Atmospheric Chemistry and Physics Discussions

References

Adebiyi, A. A. and Zuidema, P.: The role of the southern African easterly jet in modifying the southeast Atlantic aerosol and cloud environments, Quarterly Journal of the Royal Meteorological Society, 142, 1574–1589, https://doi.org/10.1002/qj.2765, 2016.

Adebiyi, A. A. and Zuidema, P.: Low cloud cover sensitivity to biomass-burning aerosols and meteorology over the Southeast Atlantic, Journal of Climate, 31, 4329–4346, https://doi.org/10.1175/JCLI-D-17-0406.1, 2018.

Adebiyi, A. A., Zuidema, P., and Abel, S. J.: The convolution of dynamics and moisture with the presence of shortwave absorbing aerosols over the southeast Atlantic, Journal of Climate, 28, 1997–2024, https://doi.org/10.1175/JCLI-D-14-00352.1, 2015.

Albrecht, B. a.: Aerosols, Cloud Microphysiscs and Fractional Cloudiness, Science, 245, 1227–1230, https://doi.org/10.1126/science.245.4923.1227, 1989.

Brioude, J., Cooper, O. R., Feingold, G., Trainer, M., Freitas, S. R., Kowal, D., Ayers, J., Prins, E., Minnis, P., McKeen, S. A., Frost, G. J., and Hsie, E.-Y.: Effect of biomass burning on marine stratocumulus clouds off the California coast, Atmospheric Chemistry and Physics Discussions, 9, 14 529–14 570, https://doi.org/10.5194/acpd-9-14529-2009, 2009.

Chazette, P., Flamant, C., Totems, J., Gaetani, M., Smith, G., Baron, A., Landsheere, X., Desboeufs, K., Doussin, J. F., and Formenti, P.: Evidence of the complexity of aerosol transport in the lower troposphere on the Namibian coast during AEROCLO-sA, Atmospheric Chemistry and Physics, 19, 14 979–15 005, https://doi.org/10.5194/acp-19-14979-2019, 2019.

Costantino, L. and Bréon, F. M.: Aerosol indirect effect on warm clouds over South-East Atlantic, from co-located MODIS and CALIPSO observations, Atmospheric Chemistry and Physics, 13, 69–88, https://doi.org/10.5194/acp-13-69-2013, 2013.

De Graaf, M., Schulte, R., Peers, F., Waquet, F., Gijsbert Tilstra, L., and Stammes, P.: Comparison of south-east Atlantic aerosol direct radiative effect over clouds from SCIAMACHY, POLDER and OMI-MODIS, Atmospheric Chemistry and Physics, 20, 6707–6723, https://doi.org/10.5194/acp-20-6707-2020, 2020.

Deaconu, L. T., Ferlay, N., Waquet, F., Peers, F., Thieuleux, F., and Goloub, P.: Satellite inference of water vapour and above-cloud aerosol combined effect on radiative budget and cloud-Top processes in the southeastern Atlantic Ocean, Atmospheric Chemistry and Physics, 19, 11 613–11 634, https://doi.org/10.5194/acp-19-11613-2019, 2019.

Devasthale, A. and Thomas, M. A.: A global survey of aerosol-liquid water cloud overlap based on four years of CALIPSO-CALIOP data, Atmospheric Chemistry and Physics, 11, 1143–1154, https://doi.org/10.5194/acp-11-1143-2011, 2011.

Dubovik, O., Holben, B., Eck, T. F., Smirnov, A., Kaufman, Y. J., King, M. D., Tanré, D., and Slutsker, I.: Variability of absorption and optical properties of key aerosol types observed in worldwide locations, Journal of the Atmospheric Sciences, 59, 590–608, https://doi.org/10.1175/1520-0469(2002)059<0590:voaaop>2.0.co;2, 2002.

Formenti, P., D'Anna, B., Flamant, C., Mallet, M., Piketh, S. J., Schepanski, K., Waquet, F., Auriol, F., Brogniez, G., Burnet, F., Chaboureau, J. P., Chauvigné, A., Chazette, P., Denjean, C., Desboeufs, K., Doussin, J. F., Elguindi, N., Feuerstein, S., Gaetani, M., Giorio, C., Klopper, D., Mallet, M. D., Nabat, P., Monod, A., Solmon, F., Namwoonde, A., Chikwililwa, C., Mushi, R., Welton, E. J., and Holben, B.: The aerosols, radiation and clouds in southern Africa field campaign in Namibia overview, illustrative observations, and way forward, Bulletin of the American Meteorological Society, 100, 1277–1298, https://doi.org/10.1175/BAMS-D-17-0278.1, 2019.

Fuchs, J., Cermak, J., Andersen, H., Hollmann, R., and Schwarz, K.: On the Influence of Air Mass Origin on Low-Cloud Properties in the Southeast Atlantic, Journal of Geophysical Research: Atmospheres, 122, 11,076–11,091, https://doi.org/10.1002/2017JD027184, 2017.

https://doi.org/10.5194/acp-2020-1089
Preprint. Discussion started: 22 October 2020

Haywood, J. M., Osborne, S. R., Francis, P. N., Keil, A., Formenti, P., Andreae, M. O., and Kaye, P. H.: The mean physical and optical properties of regional haze dominated by biomass burning aerosol measured from the C-130 aircraft during SAFARI 2000, Journal of Geophysical Research D: Atmospheres, 108, https://doi.org/10.1029/2002jd002226, 2003.

Haywood, J. M., Osborne, S. R., and Abel, S. J.: The effect of overlying absorbing aerosol layers on remote sensing retrievals of cloud effective radius and cloud optical depth, Quarterly Journal of the Royal Meteorological Society, 130, 779–800, https://doi.org/10.1256/qj.03.100, 2004.

Henderson, D. S., L'ecuyer, T., Stephens, G., Partain, P., and Sekiguchi, M.: A multisensor perspective on the radiative impacts of clouds and aerosols, Journal of Applied Meteorology and Climatology, 52, 853–871, https://doi.org/10.1175/JAMC-D-12-025.1, 2013.

Herbert, R. J., Bellouin, N., Highwood, E. J., and Hill, A. A.: Diurnal cycle of the semi-direct effect from a persistent absorbing aerosol layer over marine stratocumulus in large-eddy simulations, Atmospheric Chemistry and Physics, 20, 1317–1340, https://doi.org/10.5194/acp-20-1317-2020, 2020.

Hersbach, H., Bell, B., Berrisford, P., Hirahara, S., Horányi, A., Muñoz-Sabater, J., Nicolas, J., Peubey, C., Radu, R., Schepers, D., Simmons, A., Soci, C., Abdalla, S., Abellan, X., Balsamo, G., Bechtold, P., Biavati, G., Bidlot, J., Bonavita, M., De Chiara, G., Dahlgren, P., Dee, D., Diamantakis, M., Dragani, R., Flemming, J., Forbes, R., Fuentes, M., Geer, A., Haimberger, L., Healy, S., Hogan, R. J., Hólm, E., Janisková, M., Keeley, S., Laloyaux, P., Lopez, P., Lupu, C., Radnoti, G., de Rosnay, P., Rozum, I., Vamborg, F., Villaume, S., and Thépaut, J. N.: The ERA5 global reanalysis, Quarterly Journal of the Royal Meteorological Society, 146, 1999–2049, https://doi.org/10.1002/qj.3803, 2020.

Hill, A., Dobbie, S., and Yin, Y.: The impact of aerosols on non-precipitationg marine stratocumulus. I: Model description and prediction of the indirect effect., Quarterly Journal of the Royal Meteorological Society, 134, 1143–1154, https://doi.org/10.1002/qj.278, 2008.

Ichoku, C., Remer, L. A., Kaufman, Y. J., Levy, R., Chu, D. A., Tanré, D., and Holben, B. N.: MODIS observation of aerosols and estimation of aerosol radiative forcing over southern Africa during SAFARI 2000, Journal of Geophysical Research D: Atmospheres, 108, 1–13, https://doi.org/10.1029/2002jd002366, 2003.

Johnson, B. T., Shine, K. P., and Forster, P. M.: The semi-direct aerosol effect: Impact of absorbing aerosols on marine stratocumulus, Quarterly Journal of the Royal Meteorological Society, 130, 1407–1422, https://doi.org/10.1256/qj.03.61, 2004.

Kacenelenbogen, M. S., Vaughan, M. A., Redemann, J., Young, S. A., Liu, Z., Hu, Y., Omar, A. H., Leblanc, S., Shinozuka, Y., Livingston, J., Zhang, Q., and Powell, K. A.: Estimations of global shortwave direct aerosol radiative effects above opaque water clouds using a combination of A-Train satellite sensors, Atmospheric Chemistry and Physics, 19, 4933–4962, https://doi.org/10.5194/acp-19-4933-2019, 2019.

Kar, J., Vaughan, M., Tackett, J., Liu, Z., Omar, A., Rodier, S., Trepte, C., and Lucker, P.: Swelling of transported smoke from savanna fires over the Southeast Atlantic Ocean, Remote Sensing of Environment, 211, 105–111, https://doi.org/10.1016/j.rse.2018.03.043, https://doi.org/10.1016/j.rse.2018.03.043, 2018.

Kim, M. H., Omar, A. H., Tackett, J. L., Vaughan, M. A., Winker, D. M., Trepte, C. R., Hu, Y., Liu, Z., Poole, L. R., Pitts, M. C., Kar, J., and Magill, B. E.: The CALIPSO version 4 automated aerosol classification and lidar ratio selection algorithm, Atmospheric Measurement Techniques, 11, 6107–6135, https://doi.org/10.5194/amt-11-6107-2018, 2018.

Klein, S. A. and Hartmann, D. L.: The seasonal cycle of low stratiform clouds, Journal of Climate, https://doi.org/10.1175/1520-0442(1993)006<1587:TSCOLS>2.0.CO;2, 1993.

Lebsock, M. D., L'Ecuyer, T. S., and Pincus, R.: An Observational View of Relationships Between Moisture Aggregation, Cloud, and Radiative Heating Profiles, Surveys in Geophysics, 38, 1237–1254, https://doi.org/10.1007/s10712-017-9443-1, 2017.

https://doi.org/10.5194/acp-2020-1089
Preprint. Discussion started: 22 October 2020

Omar, A. H., Winker, D. M., Kittaka, C., Vaughan, M. A., Liu, Z., Hu, Y., Trepte, C. R., Rogers, R. R., Ferrare, R. A., Lee, K. P., Kuehn, R. E., and Hostetler, C. A.: The CALIPSO automated aerosol classification and lidar ratio selection algorithm, Journal of Atmospheric and Oceanic Technology, 26, 1994–2014, https://doi.org/10.1175/2009JTECHA1231.1, 2009.

Schulz, M., Textor, C., Kinne, S., Balkanski, Y., Bauer, S., Berntsen, T., Berglen, T., Boucher, O., Dentener, F., Guibert, S., Isaksen, I. S. A., Iversen, T., Koch, D., Kirkevåg, A., Liu, X., Montanaro, V., Myhre, G., Penner, J. E., Pitari, G., Reddy, S., Seland, Ø., Stier, P., and Takemura, T.: Radiative forcing by aerosols as derived from the AeroCom present-day and pre-industrial simulations, Atmospheric Chemistry and Physics Discussions, 6, 5095–5136, https://doi.org/10.5194/acpd-6-5095-2006, 2006.

Twomey, S.: The influence of pollution on the shortwave albedo of clouds., J.Atmos. Sci., 34, 1149–1152, 1977.

Wilcox, E. M.: Stratocumulus cloud thickening beneath layers of absorbing smoke aerosol, Atmospheric Chemistry and Physics, 10, 11 769–11 777, https://doi.org/10.5194/acp-10-11769-2010, 2010.

Winker, D. M., Vaughan, M. A., Omar, A., Hu, Y., Powell, K. A., Liu, Z., Hunt, W. H., and Young, S. A.: Overview of the CALIPSO mission and CALIOP data processing algorithms, Journal of Atmospheric and Oceanic Technology, 26, 2310–2323, https://doi.org/10.1175/2009JTECHA1281.1, 2009.

Wood, R.: Stratocumulus clouds, https://doi.org/10.1175/MWR-D-11-00121.1, 2012.

Yamaguchi, T., Feingold, G., Kazil, J., and McComiskey, A.: Stratocumulus to cumulus transition in the presence of elevated smoke layers, Geophysical Research Letters, 42, 10 478–10 485, https://doi.org/10.1002/2015GL066544, 2015.

Zhang, W., Deng, S., Luo, T., Wu, Y., Liu, N., Li, X., Huang, Y., and Zhu, W.: New global view of above-cloud absorbing aerosol distribution based on CALIPSO measurements, Remote Sensing, 11, https://doi.org/10.3390/rs11202396, 2019.

Zhou, X., Ackerman, A. S., Fridlind, A. M., Wood, R., and Kollias, P.: Impacts of solar-absorbing aerosol layers on the transition of stratocumulus to trade cumulus clouds, Atmospheric Chemistry and Physics, 17, 12 725–12 742, https://doi.org/10.5194/acp-17-12725-2017, 2017.